Regulation of antiviral responses by RIG-I dissociation from dsRNA

Jung Hyun Im

Table of contents:

Chapter 5:

Chapter 6:

ABSTRACT

Retinoic acid-inducible gene I (RIG-I) is one of RIG-I-like receptors (RLRs) together with melanoma differentiation-associated protein 5 (MDA5), and laboratory of genetics and physiology 2 (LGP2). RIG-I is the most front-line cytoplasmic viral RNA sensor and induces antiviral immune responses, such as type I interferon (IFN) production. Interestingly, although RIG-I is able to bind with double-stranded RNA (dsRNA) irrespective of size, RIG-I is activated only by short dsRNA (<500 bp) to elicit antiviral response, but not by long dsRNA (>500 bp). However, the reason of length-dependent RIG-I signaling still remains elusive.

Here, my doctoral research demonstrated that RIG-I bound to long dsRNA with slow kinetics. Remarkably, RIG-I/short dsRNA complex rapidly dissociated in an ATP hydrolysis-dependent manner, whereas RIG-I/long dsRNA was stable and rarely dissociate. Indeed, my research proposed that the RIG-I dissociation from RIG-I/dsRNA complex could be a critical step for antiviral signaling. Dissociated RIG-I exhibited homo-oligomerization, acquiring ability of physical association with mitochondrial antiviral signaling protein (MAVS), and biological activity upon introduction into living cells. Consequentially, this study herein revealed common and unique mechanisms of length-dependent recognition of dsRNA by RIG-I.

ABBREVIATIONS

RIG-I	Retinoic acid-inducible gene I
RLRs	RIG-I-like receptors
MDA5	Melanoma differentiation-associated protein 5
LGP2	Laboratory of genetics and physiology 2
IFN	Interferon
dsRNA	double-stranded RNA
ATP	Adenosine triphosphate
MAVS	Mitochondrial antiviral signaling protein
cDC	Conventional dendritic cells
CTD	C-terminal domain
CARD	Caspase activation and recruitment domain
IRF-3	Interferon regulatory factor-3
NF-κB	Nuclear factor kappa B
ssRNA	single stranded RNA
ppp	triphosphate
pp	diphosphate
PAMPs	Pathogen-associated molecular patterns
EMCV	Encephalomyocarditis virus
DMEM	Dulbecco's modified Eagle's medium
FBS	Fetal bovine serum
MEM	Minimum essential medium
DTT	Dithiothreitol

E.coli	*Escherichia coli*
IPTG	Isopropyl-β-D-thiogalactoside
DOC	Sodium deoxycholate
PDVF	Polyvinylidene difluoride
PCR	Polymerase chain reaction
KO	Knockout
KD	Knockdown
LMW	Low molecular weight
HMW	High molecular weight
AMP-PNP	Adenylyl-imidodiphosphate
AFM	Atomic force microscope
siRNA	Small interfering RNA

Chapter 1

Introduction

Introduction

1.1 RLRs

The innate immune system is systemized to react against viral infections as the first-defence mechanism of host together with the adaptive immune system. Several cytoplasmic sensor proteins detect viral RNA and elicit antiviral signals upon viral invasion. RIG-I-like receptors (RLRs) are the most front-line viral RNA sensing proteins in cytoplasm and ubiquitously expressed in almost every type of cells[1]. Therefore, many cases have been reported that deficiency of RLRs caused severe immune disorders[2,3]. RLRs-knockout mice lost the function of detecting viral RNAs in fibroblast, and conventional dendritic cells (cDC).

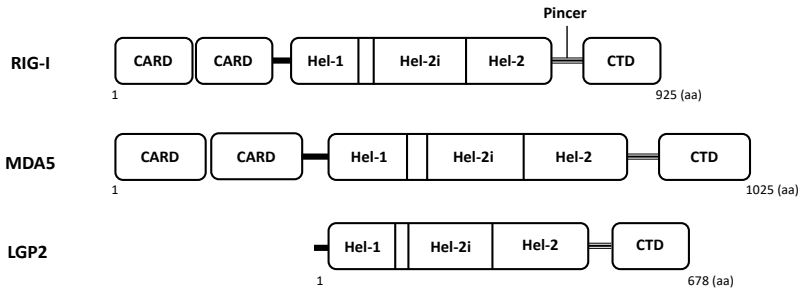

Figure 1. RLRs structure

RLRs consist of three members: retinoic acid-inducible gene I (RIG-I), melanoma differentiation-associated protein 5 (MDA5), and laboratory of genetics and physiology 2 (LGP2)[4–6]. RIG-I and MDA5 are structurally sharing conserved sequence and showing functional similarities (Figure 1). These two sensing proteins detect and bind to viral RNA using C-terminal domain (CTD) and DExD/H box

helicase domain. Moreover, both RIG-I and MDA5 induce valid defensive immune signals by releasing oligomerized N-terminal caspase activation and recruitment domain (CARD) [4,7]. Then, under the activated signals, oligomerized CARD of RIG-I or MDA5 induces CARD-CARD interaction with another CARD-containing mitochondrial antiviral signaling protein (MAVS) to trigger downstream signaling cascade including activation of interferon regulatory factor (IRF-3), nuclear factor kappa B (NF-κB) and type I interferon (IFN) ultimately [8,9] (Figure 2). On the other hand, LGP2 is unable to transmit active immune responses to downstream due to the lack of CARD, although LGP2 recognizes viral RNA with higher affinity than RIG-I and MDA5[10] (Figure 1). Additionally, LGP2 has been regarded as a protein, which positively supports RIG-I or MDA5 signaling rather than provoking antiviral signaling by itself [4,11].

1.2 Mechanism of RIG-I signaling

RIG-I and MDA5 have quite homologous structure and function in terms of leading to antiviral immune signal cascade by recognition of viral RNA[12,13]. These two cytoplasmic sensors, however, possess very distinct signal transduction properties respectively, such as RNA ligands they target, and the methods of conformation changes upon active signaling. Naïve RIG-I generally retains closed-conformation in the cytoplasm until viral RNAs were detected. As soon as RIG-I recognizes its ligands by DExD/H box helicase domain and CTD[14,15], RIG-I approaches and binds through terminal of ligand RNAs[16, 27]. Then, at roughly the same time, closed-structure

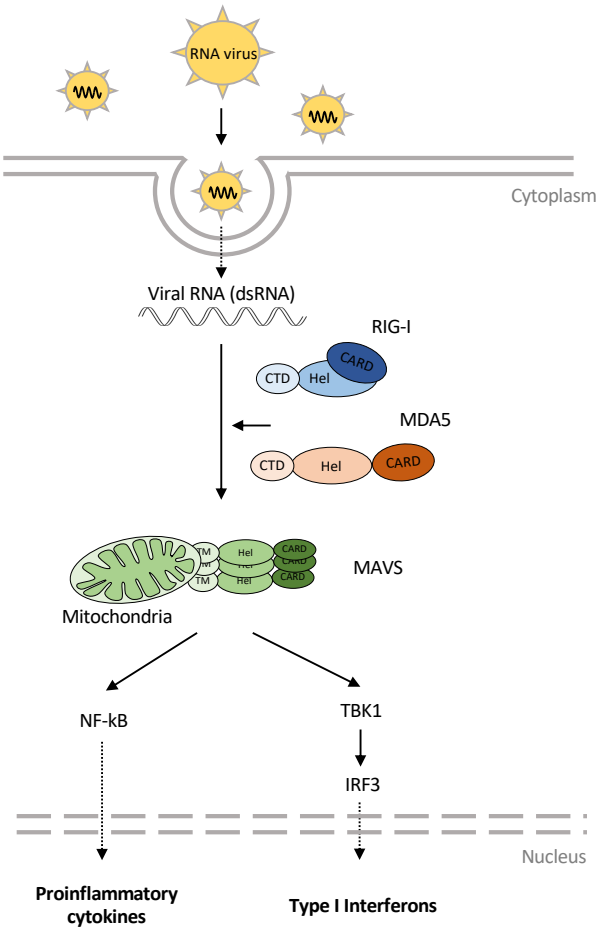

Figure 2. RIG-I and MDA5 antiviral signaling pathway

of RIG-I turned to be active formation by dramatical releasing CARD, and RIG-I exhibits ATP-driven translocation toward another terminus of RNAs with cooperative association[17,18]. In addition to conformation changes, CARD is also oligomerized, resulting in physical connection with CARD of MAVS to transmit signals[8,19]. Previous research has demonstrated that RIG-I exhibited the conformational changes upon infection of paramyxovirus, rhabdovirus, influenza virus, and Japanese encephalitis virus. Also, dengue virus and reovirus are targeted by both of RIG-I and MDA5[3,20]. That is, only specific types of RNA induce immune responses due to the activation of RIG-I, even though RIG-I is possible to bind to almost every type of

RNA except 5'OH-single stranded RNA (ssRNA)[14]. In the early stage of RIG-I study, the 5'tri- or 5'di-phosphate (5'ppp or 5'pp) structure, which is a representative pathogen-associated molecular patterns (PAMPs), has been considered only necessary condition to be the RIG-I ligand[21,22]. In fact, further researches corrected that 5'ppp or 5'pp termini are not enough to lead RIG-I activation, but additional dsRNA structure is significant because they found that artificially synthesized 5'ppp-ssRNA, which doesn't form the panhandle structure, was unable to activate RIG-I[23,24]. Conversely, dsRNA was reported as a RIG-I agonist regardless of 5'-ppp structure. However, in recent studies, it was also demonstrated that RIG-I is not able to induce antiviral responses with long dsRNA (>500 bp), but short dsRNA (<500 bp) has been regarded as strong RIG-I-stimulatory ligand although RIG-I binds to any size of dsRNA[25,26]. Collectively, RIG-I recognizes short dsRNA, and panhandle structure-formable ssRNA including tri- or di-phosphate termini.

1.3 Mechanism of MDA5 signaling

Together with RIG-I, MDA5 has the critical role of cytoplasmic sensor of viruses. Unlike RIG-I, naïve MDA5 is in stretched conformation possibly with partially exposed CARD. By AFM, 3 or 4 structural domains were relatively clearly observed, whereas RIG-I appears as round shape structure[27,28]. This is consistent with the observation that MDA5 shows basal activity in over expression in cell, but basal activity of RIG-I is undetectable [1,29]. In addition to the distinct cytoplasmic state of MDA5, MDA5 showed much less affinity to dsRNA and 5'ppp-RNA than the other RLR family members did due to the flatter surface of the RNA binding pocket on

CTD[10]. Furthermore, it is difficult to specify properties of MDA5 agonists in contrast to RIG-I, but the long dsRNA strongly induces MDA5-realted active immune responses[25]. Indeed, MDA5 has been responsible the induction of a synthetic analogue of viral dsRNA, poly (I:C), -derived immune response, but not artificially generated 5'ppp ssRNA. Since MDA5 differently recognized viral RNAs compare to RIG-I does, MDA5 reacts to specific type of viruses, such as picornavirus including Theiler's virus and encephalomyocarditis virus (EMCV)[3,30–32].

When MDA5 senses its ligand RNAs, MDA5 showed direct association on anywhere of dsRNA, so terminus of RNA didn't affect to the association[16]. In addition, ATP hydrolysis facilitates cooperative MDA5 association and oligomerization on RNA. Indeed, recent research have reported that MDA5 polymerizes along the length of long dsRNA to form fiber-like polymers with assistance of LGP2, and oligomerized MDA5 dissociated from dsRNA and interacted with MAVS[27]. Therefore, it was demonstrated that the formation of long fiber is the critical step for molding MDA5 into the active conformation.

Taken together, RIG-I can be activated by short dsRNA with or without 5'ppp-end. Also, for long dsRNA detection by MDA5, it has been reported that formation of fiber-like polymer with long dsRNA is critical for MDA5-derived signaling. However, the reason why RIG-I is not activated by binding with long dsRNA was still elusive.

1.4 Aim of this study

Accordingly, in this study, I delineated the mechanisms of dsRNA length-dependent RIG-I signaling using different length of poly (I:C). Furthermore, I demonstrated how efficiency of association and dissociation of RIG-I influences downstream signals including the dimerization of IRF-3 and induction of *IFNB* expression.

Chapter 2

Material and methods

Material and methods

2.1 Cell culture

293T (#CRL-3216, ATCC) (female), 293T MDA5 KO and HeLa cells (#CCL-2.2, ATCC) (female) were maintained in Dulbecco's modified Eagle's medium (DMEM) (Nacalai Tesque) supplemented with 10% fetal bovine serum (FBS) and 1 % penicillin/streptomycin. 293T with MDA5 KO was generated by using CRISPR-cas9 system with pSpCas9(BB)-2A-GFP (PX458) backbone plasmid, supported from Dr. Feng Zhang (Addgene plasmid #48138) as a gift, containing guide RNA (MDA5 sgRNA: forward 5'-TGGTTGGACTCGGGAATTCG-3' reverse 5'-CGAATTCCCGAGTCCAACCA-3'). SH800 cell sorter (Sony) sorted plasmid transfected 293T using GFP signal by and subjected to single-cell selection. Selected cells were cultured as a single clone. For generating MDA5 KD HeLa cells, Lipofectamine RNAiMAX Reagents (Invitrogen) was used as transfection reagent. siMDA5 (Invitrogen, #79534603) were transfected into HeLa cells for overnight, and knockdown effect was confirmed by SDS-PAGE followed by immunoblotting. L929 cells (#CCL-1, ATCC) were maintained in minimum essential medium (MEM) (Nacalai Tesque) supplemented with 10% FBS and 1 % penicillin/streptomycin.

2.2 Poly (I:C)

For generating various length of poly (I:C), commercial poly (I:C) (HMW, GE Healthcare) was treated with RNase III (New England Biolabs). HMW poly (I:C) was digested in the reaction mixture (10 μl, 10 μg poly (I:C), 0.75 units RNase III) according to the manufacturer's protocol at 37°C. The reaction was terminated by the addition of EDTA. Digested poly (I:C) was recovered using phenol/chloroform extraction and ethanol precipitation.

2.3 Purification of recombinant RIG-I from insect cells

Recombinant RIG-I was produced by baculovirus expression system. High five cells (insect cells) were infected with recombinant baculovirus expressing 6xHis-Flag RIG-I[7] and cultured in SF-900II serum free medium (Invitrogen) supplemented with 1% penicillin/streptomycin. After 72 hours infection, RIG-I protein was bound to Ni-Sepharose 6 Fast Flow beads (GE Healthcare) in binding buffer (10 mM imidazole, 50 mM Tris-HCl (pH 8.0), 150 mM NaCl, 5 mM $MgCl_2$ and 1.5 mM DTT) and eluted in elution buffer containing 500 mM imidazole. Imidazole was removed using PD-10 desalting column (GE Healthcare).

2.4 Trypsin digestion of RIG-I (insect cells)

A total of 2.7 μg Flag-tagged RIG-I in the absence or presence of different lengths of poly (I:C) (2.7 μg) was incubated at 37°C for 30 min in 10 μl of binding buffer (20 mM Tris-HCl (pH 8.0), 1.5 mM $MgCl_2$, 70 mM KCl and 1.5 mM DTT) and then treated with 165 ng TPCK (N-p-Tosyl-L-phenylalanyl chloromethyl keton)-treated trypsin from bovine pancreas (Sigma-Aldrich) at 37°C for 5 min. Trypsin digestion was stopped by adding 2x SDS sample buffer and boiling for 5 min. The samples were subjected to SDS-PAGE followed by immunoblotting with anti-human RIG-I monoclonal antibody (clone N3514, epitope: aa218-792) [14].

2.5 Purification of recombinant RIG-I protein from 293T cells

293T cells ($1x10^6$ cells) were transfected with 5 μg of the expression plasmid pEF-BOS-Flag RIG-I[4] or pEF-Flag RIG-I K270A[4] by using Polyethylenimine Max (Polysciences). After overnight transfection, the cell extract was prepared with lysis buffer (20 mM Tris–HCl (pH 7.5), 150 mM NaCl, and 1% NP-40 supplemented with protease inhibitors cocktail). The cell lysate was incubated with anti-Flag antibody immobilized to magnetic beads at 4°C for 16 hours. Beads were washed 3 times with lysis buffer and RIG-I was eluted by incubation with of 3x Flag peptide at room temperature for 30 min. During incubation time, the sample was mixed by tapping every 10 min. The supernatant was used as naïve RIG-I (293T cells).

To isolate dissociated RIG-I from cells, MDA5 KO 293T cells were transfected with 10 μg of pEF-BOS- Flag RIG-I using Polyethylenimine Max. After overnight transfection, 5 μg of LMW poly (I:C) was transfected into the cells for 3 hours. Cell lysate was prepared and incubated with magnetic beads coupled with anti-dsRNA antibody at 4°C for 16 hours. Beads were washed 3 times with lysis buffer and mixed with 1 mM ATP at 37°C for 30 min. Dissociated RIG-I was recovered from the supernatant.

2.6 Association and dissociation assays for RIG-I-Poly (I:C) complex

Association and dissociation assays were performed with binding buffer (20 mM Tris-HCl (pH 8.0), 1.5 mM $MgCl_2$, 70 mM KCl and 1.5 mM DTT) at 37°C for the indicated time. To isolate RIG-I/poly (I:C) complexes, magnetic bead-antibody-dsRNA combination was newly designed. Protein G magnetic Dynabeads (5 μl, Thermo Fisher) were mixed with 1 μg of anti-dsRNA antibody (SCICONS, K1) at

room temperature for 40 min. Beads-antibody complexes were washed three times, then 1 μg of poly (I:C) was added and incubated at 4°C for 1 hour. For removing residual dsRNA, magnetic bead-antibody-dsRNA complexes were washed three times. Beads were incubated with 1 μg of recombinant RIG-I (insect cells) or purified RIG-I (293T cells) at 37°C to generate RIG-I-poly(I:C) complexes for the indicated times. For binding kinetics, the complexes (beads) were collected by pulling down magnetic beads and subjected to SDS-PAGE following immunoblotting with anti-Flag (RIG-I). To examine dissociation kinetics, the complexes formed for 60 min were incubated with or without 1 mM ATP for the indicated times and the complexes remained on the beads were analyzed as described above. The steps of association and dissociation were schematized below (Figure 3).

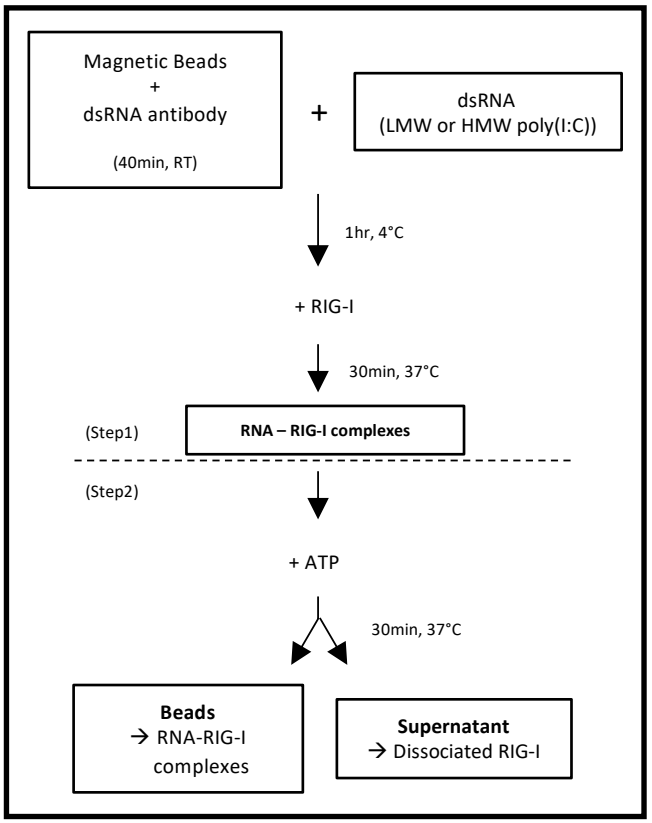

Figure 3. Scheme of association and dissociation assay

2.7 MAVS ΔTM

MAVS ΔTM was produced in *Escherichia coli (E. coli)* and purified as previously described[33]. Firstly, the MAVS ΔTM vector including target gene amplified by PCR was prepared with pEt-based GRP fusion vector and transformed into *E. coli* BL21(DE3) strain. *E. coli* was incubated at 37°C with 100 mg/ml of ampicillin for selection. Isopropyl-β-D-thiogalactoside (IPTG) treatment induced protein expression, and *E. coli* was incubated at 16°C for 16 hours. The lysate of bacteria was prepared with lysis buffer (50 mM Tris-HCl (pH.8), 500 mM NaCl, and 20 mM imidazole supplemented with protease inhibitor cocktail). The MAVS ΔTM protein bound to Ni-Sepharose 6 Fast Flow (GE Healthcare) and eluted in elution buffer containing 500 mM imidazole.

2.8 AFM

Recombinant RIG-I and HMW poly (I:C) mixed in AFM buffer (10 μl, 5 mM HEPES–NaOH pH 7.5, 50 mM NaCl and 5 mM $MgCl_2$) including 1 mM ATP was incubated at 37°C for 30 min. Then, RIG-I/HMW poly (I:C) was fixed with 0.05% glutaraldehyde at 37°C for 15 min (Nacalai Tesque) (Figure 6c). Naïve RIG-I (293T cells) and dissociated RIG-I were prepared in ATPase buffer (10 μl, 20 mM Tris–HCl pH 7.5, 1.5 mM $MgCl_2$ and 1.5 mM DTT) and incubated at 25°C for 30 min. To examine the effect of ATP treatment on RIG-I, RIG-I incubated in ATPase buffer together with 1 mM ATP at 25°C for 15 min (Figure 8). These samples were placed

on 10 mM spermidine (Nacalai Tesque) treated mica at room temperature for 15 min. The mica was washed with Milli-Q and dried thoroughly by blowing with nitrogen gas.

Multimode AFM Nanoscope IIIa and J scanner (Bruker, Veeco, Digital Instruments) were used for AFM imaging. Samples on mica were scanned with rectangular silicon cantilevers with 14 μm long tetrahedral tips (OMCL-AC160TS-C3, Olympus). Scanned images were analyzed using the software, NanoScope Analysis (v. 5.31 rl, Digital Instruments) [27].

2.9 ATPase assay

One microgram of each protein was incubated at room temperature for 10 min in 20 μl of reaction mixture including 250 ng of LWM poly (I:C), and 10x ATPase assay buffer (200 mM Tris-HCl pH 8.0, 15 mM MgCl2, 15mM DTT). 5 mM of ATP was added to the reaction mixture respectively to a final concentration of 1 mM, and these mixtures were incubated at 37°C for 30 min. Biomol Green (Enzo) was added to each sample to measure the free phosphate which was generated from reaction. After 10 min incubation at room temperature, free phosphate was measured at 630 nm of absorbance.

2.10 Native-PAGE

Naïve or dissociated RIG-I was analyzed using 3-12 % Bis-Tris Native PAGE Gels under the NativePAGE Novex Bis-Tris Gel System. Samples were

electrophoresed at 200 V at 4°C for 100 min and transferred to PVDF membranes at 15 V for 1 hour. Proteins on the membranes were fixed with 20 ml of 8% acetic acid. The membranes were rinsed according to the Native-PAGE protocol (Life Technologies). RIG-I was visualized by immunoblotting with anti-Flag antibody (RIG-I).

Native PAGE of IRF-3 was described elsewhere[34]. Protein samples were prepared with 5X Native PAGE sample buffer and loaded on the 7.5% polyacrylamide gel. The electrophoresis was performed using running buffer (25 mM Tris-HCl pH 8.4, 192 mM glycine) with or without 0.2% of sodium deoxycholate (DOC). The proteins were transferred to PDVF membranes. Dimerization of IRF-3 was visualized by immunoblotting with anti-IRF-3 antibody (CBX00167, Cosmobio).

2.11 Luciferase assay and Protein transfection

Reporter genes (0.5 μg of p-55C1BLuc and 25 ng of p-RL-TK)[4,35] were transfected into 293T cells. After 16 hours, naïve or dissociated RIG-I, isolated from MDA5 KO 293T cells, was transfected into cells using the Xfect protein transfection kit (Takara) for 2 hours. Cells were incubated for additional 4 hours in fresh medium. Luciferase activities were determined as previously described [27].

2.12 Real-Time qPCR

The RNA from cells was extracted by TRIzol (Thermo Fisher) and synthesized to cDNA using ReverTra ACE qPCR RT Master Mix including gDNA remover (TOYOBO). cDNA was mixed with primers (Table 1) and Thunderbird SYBR real-time PCR Mix (TOYOBO). Real-Time qPCR was performed and analyzed using Step One plus real-time PCR system (Applied Biosystems).

Table 1. Primer sequences for real-time PCR

Primers for human gene	Sequences (5'→ 3')
IFNB	Forward: AGCTGCAGCAGTTCCAGAAG Reverse: AGTCTCATTCCAGCCAGTGC
GAPDH	Forward: CTGCACCACCAACTGCTTAG Reverse: GTCTTCTGGGTGGCAGTGA

2.13 Artificial oligomerization of RIG-I in cells

For analysis of RIG-I oligomerization in cells, we modified an artificial homodimerization system (ARGENT Kit, ARIAD; currently iDimerize system, Clontech). We used 3 tandem repeats of mutant FK 506 Binding Protein 12 (FK_{F36V}), which can be cross-linked by the cell-permeable chemical AP20187. FK_{F36V} harbours an F36V mutation, which impairs binding affinity to the immunosuppressive agent, FK506. AP20187 was specifically designed for binding with FK_{F36V}; therefore, it didn't disturb endogenous FK binding proteins. Thus, this system specifically crosslinks a target protein without unwanted side effects. We made artificial

constructs to oligomerize full-length RIG-I in cells (FK-RIG-I). FKBP/RIG-I fusion construct was made as described[36], except full-length RIG-I was fused at C-terminus of FKBP x 3. The construct, pC4Fc3E-RIG-I was used for transfection. L929 cells (5 x 10^5 cells) were transfected with p-55C1BLuc (1.25 μg, signal reporter), pRL-TK (10 ng, reference reporter) and the expression vector (pC4Fc3E-RIG-I) (1.25 μg) for 12 hours. Cells were replated into 96 well dishes for 12 hours. Cells were stimulated with 100 ng of AP20187 for 9 hours. Reporter activities were determined by the dual luciferase assay kit as described [1].

2.14 Statistical analysis

Where applicable, the two-tailed Student's *t*-test was used as statistical analysis to compare two groups of experimental data. Also, one-way ANOVA (Analysis of Variance) followed by Tukey's post-hoc test or two-way ANOVA followed by Sidak's post-hoc test was used for multiple comparison using Prism software (version 10). Unless specified, data was expressed as mean ± standard deviation (SD) with P <0.05 being considered significant (*P<0.05, **P<0.01, ***P<0.001 and ****P<0.0001).

Chapter 3

Results

Results

3.1 *IFNB* gene activation in HeLa cells: Length-dependent recognition of poly (I:C) by RIG-I.

First, following the previous report, various sizes of poly (I:C) were generated by digestion with RNase III for the mechanistic study of the size-dependent dsRNA recognition by RIG-I (Figure 4a)[25]. The different sizes of poly (I:C) were tested their abilities to activate *IFNB* gene in HeLa cells. It has been well documented that intracellular dsRNA is essentially recognized by RIG-I and MDA5[3, 25]. Because MDA5 preferentially recognizes commercial undigested poly (I:C)[25], I knocked downed MDA5 expression prior to stimulation. Figure 4b shows knockdown efficiency for MDA5 expression by siRNA. The result confirms that the siRNA attenuated MDA5 protein levels (20% of control). MDA5 knockdown cells were transfected with various sizes of poly (I:C) (Figure 4a) and examined for *IFNB* gene expression (Figure 4c). The shortest poly (I:C) generated by 60 min RNase III digestion (termed as LMW poly (I:C), thereafter) exhibited highest *IFNB* expression. The increase in poly (I:C) size gradually attenuated their abilities to induce *IFNB* and undigested poly (I:C) (termed as HMW poly (I:C), thereafter) exhibited lowest activity (20% that of LMW poly (I:C)). These results are consistent with previous study demonstrating that long and short poly (I:C) preferentially activates MDA5 and RIG-I, respectively by using mouse fibroblast[25].

Previously, a series of synthetic dsRNA were examined for stimulation of *IFNB* gene through RIG-I[14]. The RIG-I structure after binding with these

immunostimulant dsRNA was examined by trypsin digestion. The study revealed that RIG-I conforms trypsin-resistant domain (30 kDa fragment) upon binding with these "active" dsRNA. However, binding with commercial poly (I:C) generated trypsin-resistant 66 kDa but not 30 kDa fragment[14]. This study inspired me to examine trypsin-resistant RIG-I structure upon binding with various length of poly (I:C). RIG-I was incubated with various sizes of poly (I:C) and digested with trypsin (Figure 4d). Figure 4d shows that the intensity of 66 kDa molecule decreased as the length of poly (I:C) decreased. In contrast, the intensity of 30 kDa molecule increased as the length of poly (I:C) decreased. These results suggested that lack of RIG-I activation by long dsRNA is not simply due to lack of their association. Importantly, the results suggested that RIG-I conforms distinct structure upon binding with stimulatory and non-stimulatory dsRNA.

3.2 Binding kinetics of RIG-I with HMW or LMW poly (I:C).

Next, I examined binding kinetics of RIG-I and HMW or LMW poly (I:C) by pull-down assay (Materials and methods; Figure 3). Naïve RIG-I was incubated with same mass of LMW or HMW poly (I:C) for different times and bound RIG-I was quantified (Figure 5). RIG-I bound to LMW poly (I:C) with faster kinetics and higher endpoint compared to HMW poly (I:C). The mechanism of length-dependent association of RIG-I and dsRNA will be discussed later (Discussion).

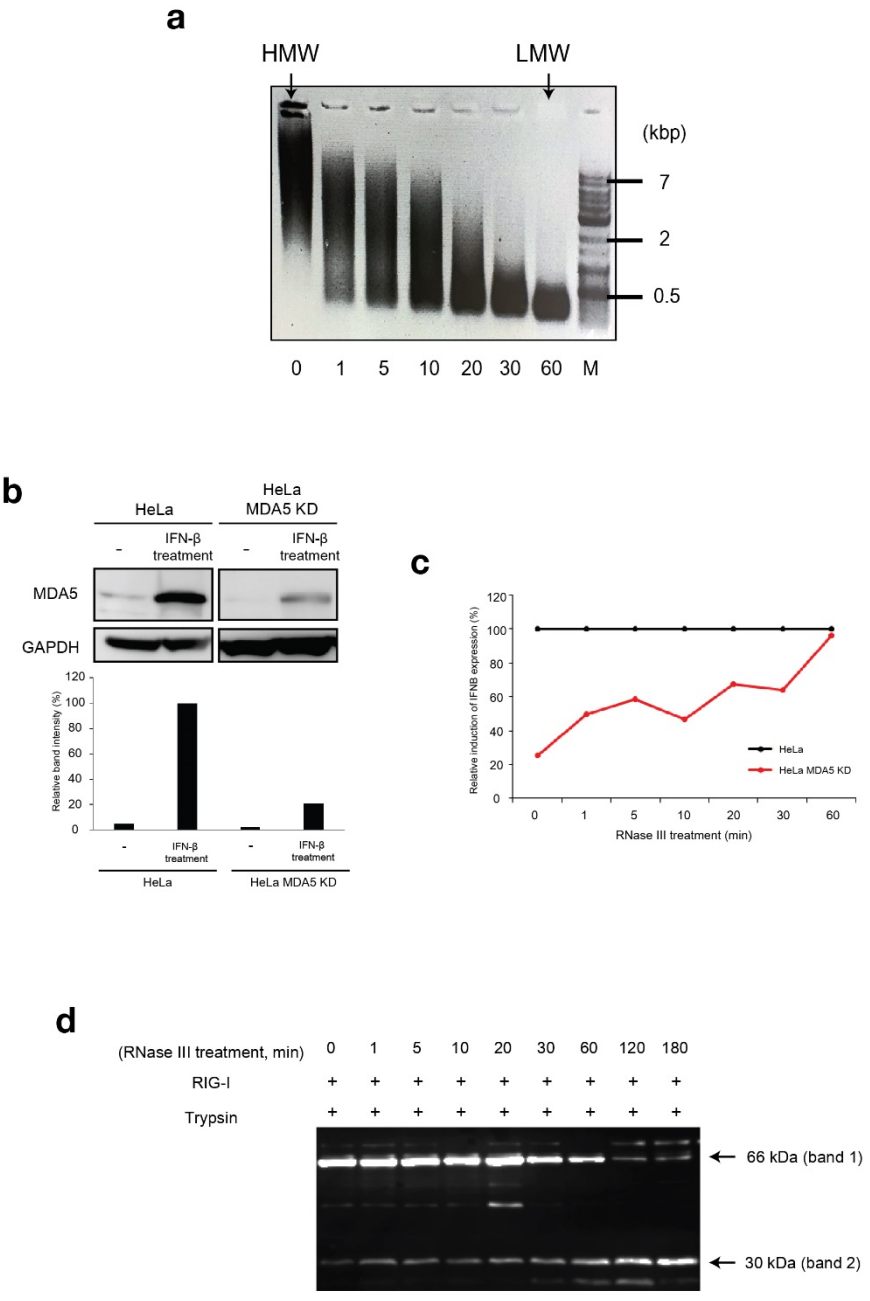

Figure 4. Poly (I:C) length-dependent binding pattern of RIG-I. (a) According to previous reports, poly (I:C) was digested by RNase III to generate various sizes of dsRNA. Commercial poly (I:C) was digested for 0, 1, 5, 10, 20, 30 and 60 min with RNase III. Undigested intact poly (I:C) was used as HMW poly (I:C), and the product obtained after 60 min of digestion was used as LMW poly (I:C). The exact experiments were performed once, and similar experiment was performed independently and showed similar results. M: DNA

marker. (b) Expression of MDA5 in WT HeLa and MDA5 KD HeLa was examined with or without IFN-β treatment. The effect of siMDA5 was confirmed twice independently (n=2). Representative image was shown (top), and the intensity of MDA5 bands were measured. The graph showed relative band intensity of MDA5 (bottom, MDA5 expression in IFN-β treated WT HeLa: 100%). (c) The different sizes of poly (I:C) obtained in (a) were used for this experiment. Duplicated wells of cells (biological duplicates, n=2) were individually transfected with different sizes of poly (I:C), and the experiment was performed once. Relative *IFNB* gene expression was calculated: the amounts of *IFNB* mRNA in wild type HeLa cells as 100 %. The graph shows mean values. (d) RIG-I binding pattern was analyzed by trypsin digestion. Recombinant RIG-I and different length of poly (I:C) generated in (a) were mixed at 37°C for 30 min. The mixture was digested with trypsin at 37°C for 5 min. The reaction mixtures were subjected to SDS-PAGE and immunoblotting with anti-RIG-I as the probe. This exact experiment was performed once, and similar experiment using different time points was performed once and showed similar results.

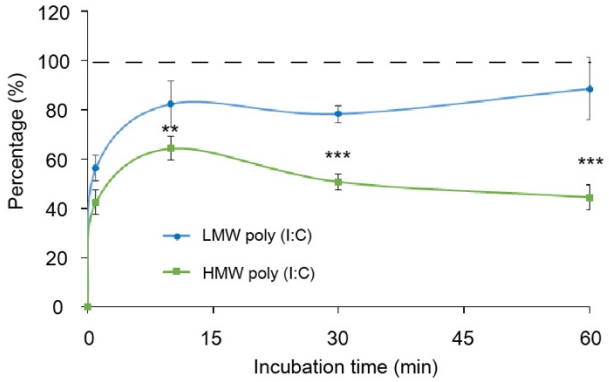

Figure 5. Association kinetics of RIG-I with HMW or LMW poly (I:C). Association kinetics between RIG-I and poly (I:C) were analyzed. Magnetic beads bound HMW or LMW poly (I:C) and RIG-I were incubated at 37 ˚C for indicated times. RIG-I/poly (I:C) complexes were recovered and analyzed by immunoblotting with anti-Flag, and then band intensity (chemical luminescence) was quantified. The three sets of experiments were performed in independent tubes. The triplicated samples were analysed once (n=3). Input RIG-I=100%. Error bar: ± SD. The significance between time-point factors, between two different poly (I:C) factors or between time x different poly (I:C) factors was confirmed by two-way ANOVA, and the data significance between two different poly (I:C) at each time-point was analyzed by Sidak's post-hoc test (**P<0.01 and ***P < 0.001).

3.3 Analyses of dissociation of RIG-I/poly (I:C) complex.

It was reported that MDA5 delivered the active antiviral signaling by dissociating from filamentous MDA5/dsRNA complex[27]. Thus, I analysed dissociation kinetics of RIG-I from LMW and HMW poly (I:C). First, complex of RIG-I with LMW or HMW poly (I:C) were formed on magnetic beads, then incubated with 1 mM of ATP. RIG-I remained on the magnetic beads was quantified (Figure 6a). The results showed that RIG-I dissociated from LMW poly (I:C) with initial 1 min incubation and gradually thereafter (80 % dissociation at 60 min) (Figure 6a). In contrast, RIG-I/HMW poly (I:C) complex dissociated less efficiently and 60 % RIG-I remain associated with HMW poly (I:C) after 60 min of incubation.

This experimental system (trap of poly (I:C)/RIG-I on magnetic beads for their association and dissociation) was applied for interaction between MDA5 and HMW poly (I:C) (Figure 6b). The result is consistent with previous notion that MDA5 efficiently binds with HMW poly (I:C) and their dissociation is promoted by ATP and LGP2[27].

Because the complex of RIG-I/HMW poly (I:C) is relatively stable compared to that of RIG-I/LMW poly (I:C), the complex was examined by AFM to explore the mechanistic insight for this (Figure 6c). HMW poly (I:C) is observed as string-like structure. Occasionally, irregular, large structures on HMW poly (I:C) were observed. This complex contrasts with the filament-like complexes formed by HMW poly (I:C) and MDA5[27]. From the size quantification, the structure corresponded to 400-2880 times volume of RIG-I monomer, suggesting that RIG-I forms large aggregates on

HMW poly (I:C) (Figure 6c). I will discuss about the nature of the multimeric complex of RIG-I in Discussion.

Next, I focus on the effect of ATP on RIG-I dissociation from LMW poly (I:C) (Figure 7). In the absence of ATP, a fraction of RIG-I (20 %) dissociated from LMW poly (I:C). In the presence of unhydrolyzable analogue, AMP-PNP, the dissociation was partially inhibited (20 to 10 %). However, in the presence of ATP, the dissociation was enhanced (20 to 45 %) (Figure 7a). To further confirm this, RIG-I dissociation was observed over time course (Figure 7b). In the absence of ATP, a fraction of RIG-I dissociated within 1 min incubation, thereafter no further dissociation was observed. In the presence of ATP, relatively rapid dissociation was observed within 10 min incubation.

Because RIG-I is a dsRNA dependent ATPase, to address the role of ATP hydrolysis, I examined an ATPase-deficient RIG-I mutant, RIG-I K270A, for dissociation. Unlike wild type RIG-I, RIG-I K270A acts as dominant inhibitor in the antiviral signaling[1]. The result of Figure 7c confirmed that wild type RIG-I exhibited ATPase activity, and it is further enhanced by LMW poly (I:C). ATPase activity of RIG-I K270A was undetectable even in the presence of LMW poly (I:C). Wild type RIG-I and RIG-I K270 were subjected to binding with LMW poly (I:C) and dissociation was examined in the presence of ATP (Figure 7d). Wild type RIG-I/ LMW poly (I:C) complex dissociated by incubation, however RIG-I K270/LMW poly (I:C) complex exhibited little dissociation. Taken together, these results suggested that unlike long poly (I:C)/RIG-I complex, short poly (I:C)/RIG-I dissociates efficiently

and that ATP hydrolysis is critical for effective induction of RIG-I dissociation from RIG-I/LMW poly (I:C) complexes.

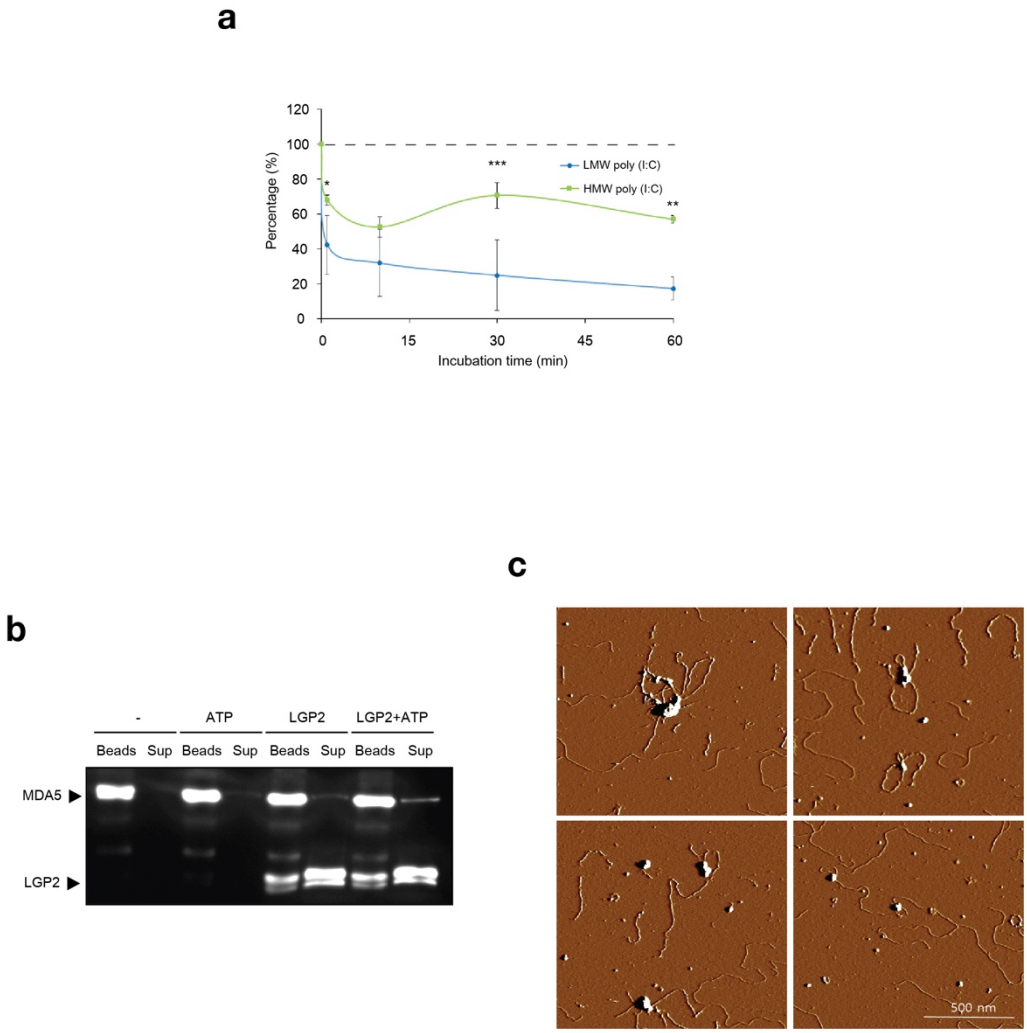

Figure 6. Dissociation kinetics of RIG-I/LMW or HMW poly (I:C). (a) RIG-I/LMW or RIG-I/HMW poly (I:C) were formed on magnetic beads as described in Figure 5 by incubation at 37˚C for 60 min. The beads were washed three times with buffer, the beads were further incubated with 1 mM of ATP at 37°C for indicated times. RIG-I bound to poly (I:C) (on magnetic beads) were analysed by immunoblotting. The dissociation kinetics was determining by quantification as in Figure 5. The three sets of experiments were performed in independent tubes. The triplicated samples were analysed once (n=3). RIG-I bound to LMW or HMW poly (I:C) after initial 60 min incubation=100%. Error bar: ± SD. The significance between time-point factors, between two different poly (I:C) factors or between time x different poly (I:C) factors was confirmed by two-way ANOVA, and the data significance between two different poly (I:C) at each time-point was analyzed by Sidak's post-hoc test (*P<0.05, **P<0.01 and ***P < 0.001). (b) Recombinant MDA5 was incubated with HMW poly (I:C) as in (a). MDA5/poly (I:C) complexes (beads) and dissociated MDA5 (supernatant) were collected respectively after additional 30 min incubation in absence or presence of ATP

or LGP2. Each sample was analyzed by immunoblotting using anti-Flag (MDA5 and LGP2). Sup: Supernatant. The experiment was performed once. (c) AFM observation of RIG-I/HMW poly (I:C) complex. RIG-I and HMW poly (I:C) were incubated at 37°C for 30 min. Four representative fields are shown from one-time experiment. For size comparison, see AFM image of naïve RIG-I in Figure 8a. Similar experiment using rice bran dsRNA was performed once, and large aggregates on long dsRNA were observed.

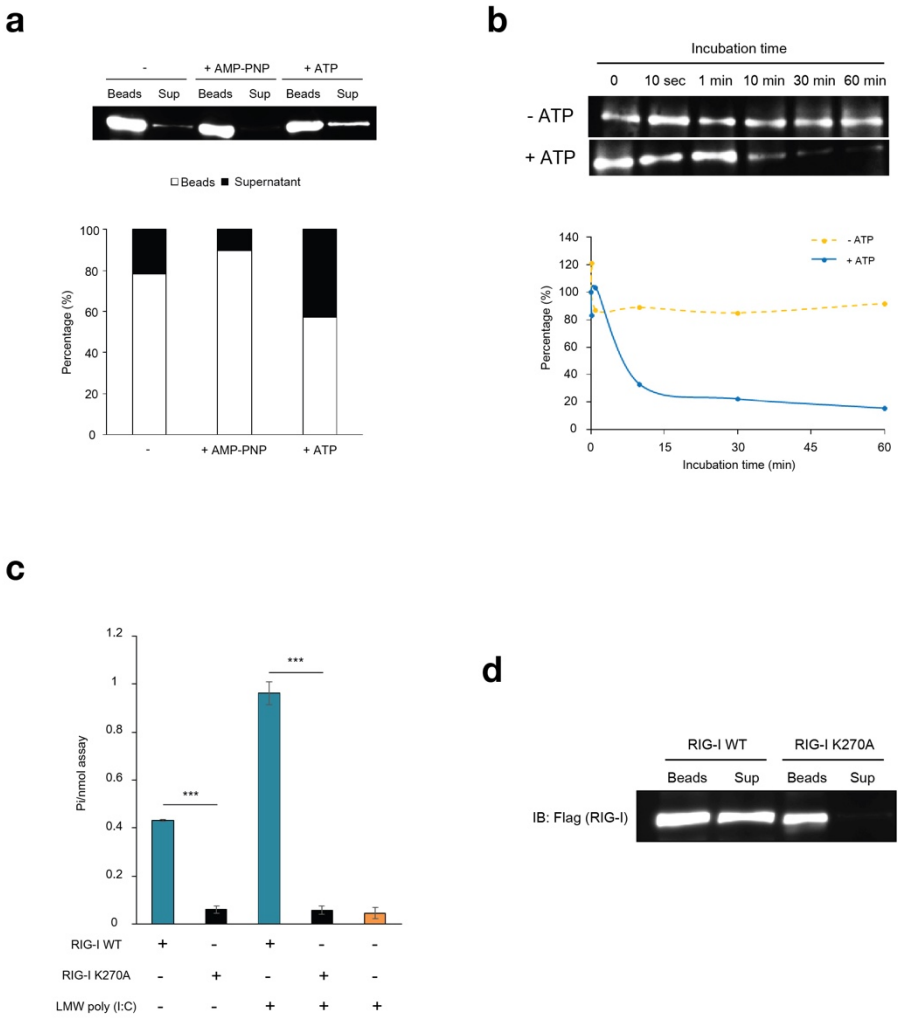

Figure 7. The effect of ATP and its hydrolysis for RIG-I from LMW poly (I:C). (a) RIG-I/LMW poly I:C) complexes were formed on magnetic beads as in Figure 5. The complexes were incubated in the absence or presence of 1 mM AMP-PNP or 1 mM ATP and RIG-I bound to magnetic beads and dissociated (in the supernatant) were analysed by immunoblotting. This exact experiment was performed once, and similar experiments were performed 2 times independently. A representative immunoblot image is shown (top). The percentage of associated and dissociated RIG-I were quantified from band intensities (chemical luminescence, bottom). (b) Dissociation rate of RIG-I with or without ATP treatment was investigated. The RIG-I/LMW poly (I:C) complexes formed on the magnetic beads were isolated and incubated in the absence or presence of 1 mM ATP at 37°C for different times. RIG-I bound to poly (I:C) (beads) was analyzed by immunoblotting as in figure 6a. The experiment was performed once. (c) RIG-I WT and RIG-I K270A were analyzed for ATPase activity in the presence or absence of LMW poly (I:C). The three sets of experiments were performed in independent tubes. The triplicated samples were analysed once (n=3). Means ± SD is indicated. ***P < 0.001, two-tailed Student's *t*-test. (d)

Dissociation of RIG-I was induced with wild-type RIG-I and ATP hydrolysis deficient RIG-I mutants, RIG-I K270A. RIG-I was incubated with LMW poly (I:C) at 37°C for 30 min respectively. RIG-I/LMW poly (I:C) complexes were collected and incubated at 37°C for 30 min with ATP. RIG-I/LMW poly (I:C) (Beads) and dissociated RIG-I (Sup) were recovered and analyzed by immunoblotting. Sup: Supernatant. The experiment was performed twice, and similar results were obtained.

3.4 AFM observation of naïve and dissociated RIG-I.

A previous study with MDA5 demonstrated that MDA5 binds to long dsRNA and dissociates in the presence of ATP and LGP2 and the dissociated MDA5 conforms active structure with exposed CARD as well as forming homo oligomers to transmit signal to subsequent signaling molecule MAVS[27]. Analogy with this, I hypothesized that RIG-I forms multimeric complexes upon dissociation from LMW poly (I:C). For further analyses, I prepared recombinant RIG-I (naïve) in human 293T cells by over expression (Materials and methods). Dissociated RIG-I was obtained through in vitro binding with LMW poly (I:C) followed by dissociation in the presence of ATP (Materials and methods). To validate my hypothesis, naïve RIG-I and dissociated RIG-I were observed by AFM (Figure 8). Unlike MDA5, which appeared as unfolded structure composed of 2-3 domains[27], naïve RIG-I appeared as a single globular shape (30.8 nm± 6.41 nm, Figure 8a, left). Because the preparation of dissociated RIG-I contained ATP used for the dissociation, naïve RIG-I was incubated with ATP alone to examine the effect of ATP (Figure 8a, middle). Incubation with ATP increased RIG-I diameter (41.14 nm ± 11.4 nm). The AFM image of dissociated RIG-I is presented in Figure 8a, right. To compare these RIG-I, 50 RIG-I images were chosen randomly, and diameter were quantified and displayed as histogram (Figure 8b). The average diameter ± SD was 30.8 nm ± 6.4 nm, 41.14 nm ± 11.4 nm and 65.1 nm ± 12.2 nm, for naïve, ATP-treated, and dissociated RIG-I, respectively (Figure 8c). Although incubation of naïve RIG-I with ATP increased in diameter, dissociated RIG-I much increased from either naïve or ATP-treated RIG-I. To further evaluate their sizes, height, and volume were quantified and statistically analyzed (Figure 8d-e).

These results suggested that dissociated RIG-I is increased in size as compared to naïve and ATP-treated RIG-I, consistent with my hypothesis that dissociated RIG-I forms multimers.

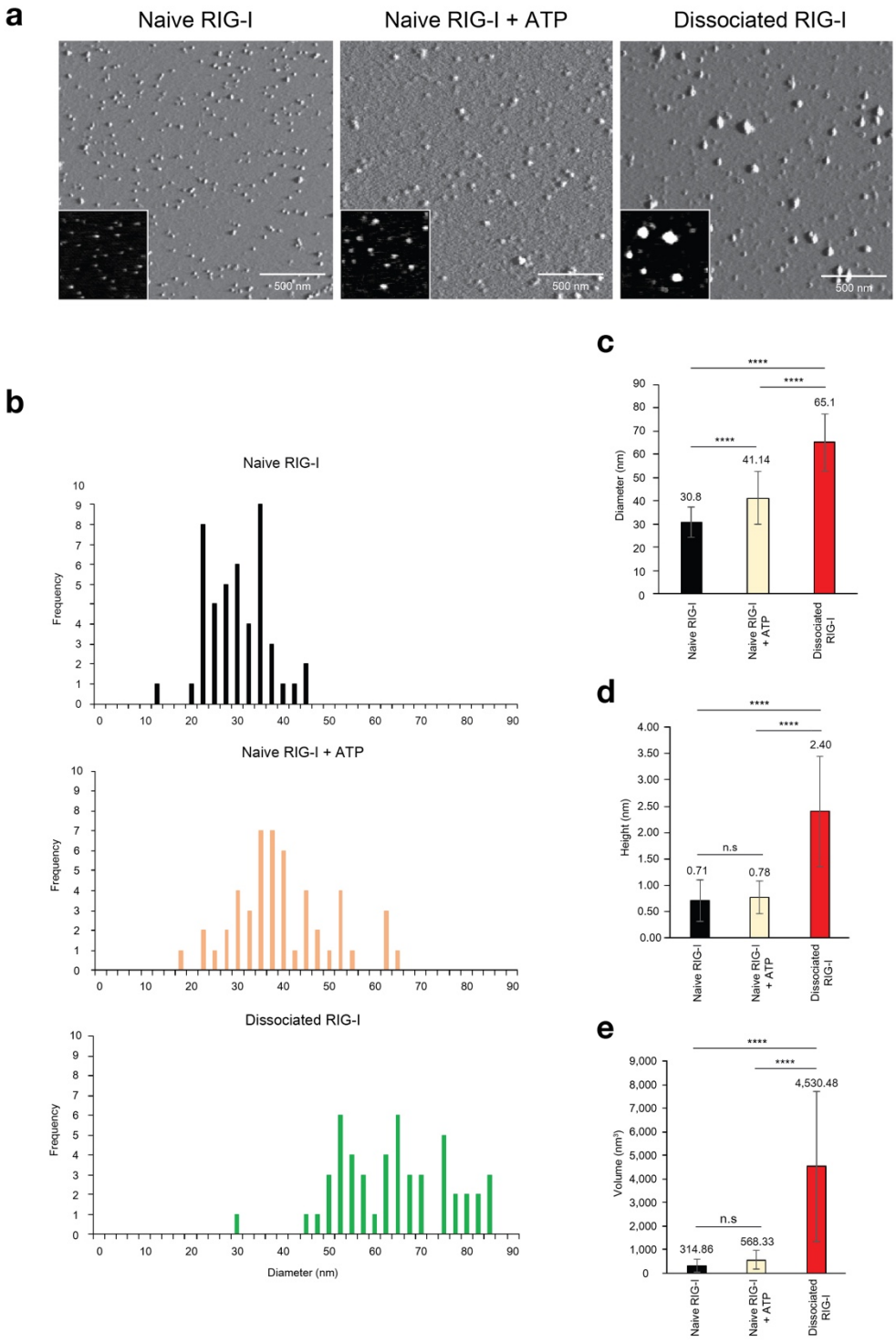

Figure 8. Conformation changes of dissociated RIG-I. (a) Different morphology of each RIG-I was analyzed by AFM. Naïve RIG-I (left) and 1 mM ATP treated RIG-I (middle) were

observed. Dissociated RIG-I was obtained by incubation of RIG-I/LMW poly (I:C) complex with 1 mM ATP treatment for 30 min. Dissociated RIG-I was recovered and subjected to AFM analysis (right). Enlarged images are shown at left bottom of each field (500 x 500 nm^2). AFM analyses of naive RIG-I and ATP-treated RIG-I were performed once. AFM analyses of dissociated RIG-I were performed twice independently, and similar images were obtained. A representative image is shown. For size quantification, 50 RIG-I proteins (white dots) were randomly chosen from each representative images, and diameter, height of each 50 RIG-I proteins were determined by a software (NanoScope Analysis). (b) Histogram of RIG-I diameter observed from AFM. (c, d) The average of diameter, height. (e) Volumes of dissociated RIG-I were calculated from diameter and height. Error bars represent ± SD (n=50). Data were analyzed using one-way ANOVA followed by Tukey's post-hoc test (n.s. not significant, ****$P < 0.0001$).

3.5 Biochemical analyses of dissociated RIG-I.

Next, dissociated RIG-I was biochemically characterized by non-denaturing polyacrylamide electrophoresis (native-PAGE, Figure 9a). Majority of naïve RIG-I was electrophoresed as fast migrating species with small amount of slow migrating species. I presume that the fast and slow migrating species as monomer and small oligomer form of RIG-I. RIG-I incubated with ATP was electrophoresed similarly as naïve RIG-I except increased small oligomers accompanied with further slow mobility fraction. On the other hand, dissociated RIG-I was mostly composed of very slow migrating species, presumably forming large oligomers.

Because dissociated RIG-I exhibited structural difference compared to naïve RIG-I (large size as determined by AFM and slow mobility in native-PAGE), I was inspired to examine if dissociated RIG-I is capable of binding with dsRNA. Naïve and dissociated RIG-I were mixed with immobilized LMW poly (I:C) and bound RIG-I was detected (Figure 9b). As expected, naïve RIG-I was efficiently recovered in the precipitate, whereas dissociated RIG-I was little recovered. This result suggests that dissociated RIG-I lost dsRNA binding property presumably due to dramatic conformational change and multimer formation.

I further hypothesized that dissociated RIG-I acquire ability to interact with subsequent signaling adaptor, MAVS. To test this, interaction between RIG-I and MAVS was examined by co-precipitation experiment (Figure 9c). The interaction between naïve RIG-I and MAVS was undetectable, suggesting that naïve RIG-I is not ready to interact because of its masked CARD. However, dissociated RIG-I exhibited

strong interaction with MAVS. Interestingly, naïve RIG-I mixed with LMW poly (I:C) exhibited a weak binding with MAVS, presumably due to small amounts of dissociated RIG-I generated during the incubation. In contrast, the interaction of MAVS and RIG-I incubated with HMW poly (I:C) was under detectable levels. These results strongly support my hypothesis that dissociated RIG-I is solely the signaling competent form.

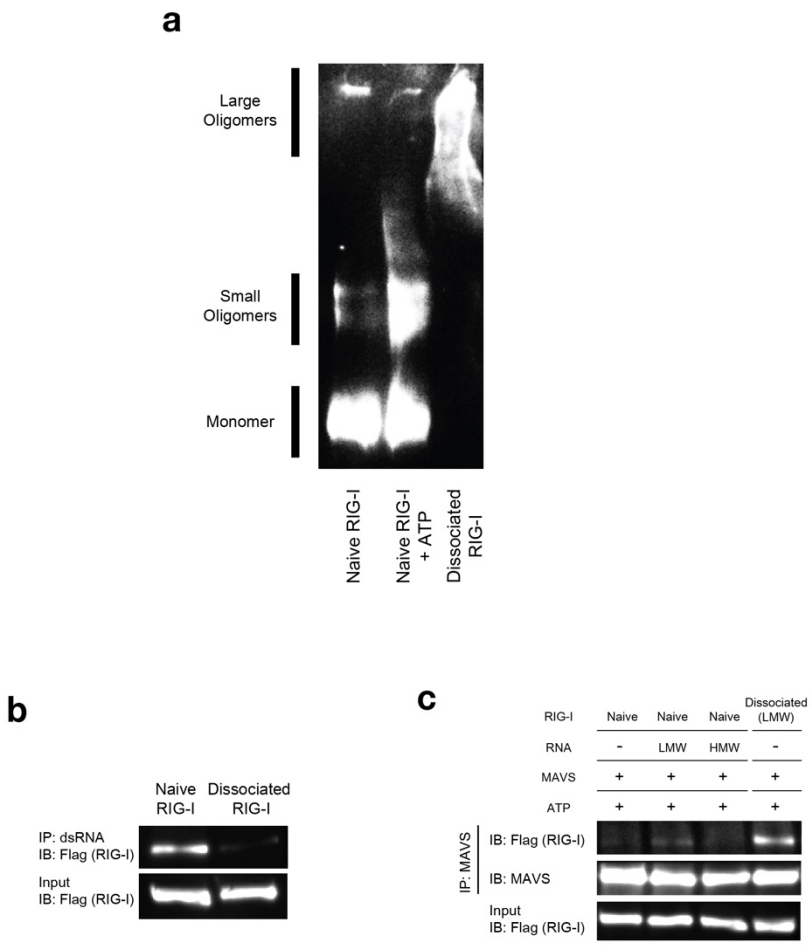

Figure 9. Biochemical analysis of large RIG-I oligomers. (a) The samples in (Figure 8), naïve RIG-I (293T) in the absence or presence of 1 mM ATP and dissociated RIG-I were prepared and subjected to native-PAGE and analysed by immunoblotting. The positions of monomers, small oligomers and large oligomers are indicated. The exact experiment was performed once and similar experiment was independently performed once, and similar results were obtained. (b) Association ability of naïve or dissociated RIG-I to LMW poly (I:C) was investigated. Recombinant naïve and dissociated RIG-I (20 ng each) were applied to association assay with LMW poly (I:C). After incubation at 37°C for 30 min, RIG-I/LMW poly (I:C) complexes (beads) were analyzed by immunoblotting (IP: dsRNA; IB: Flag (RIG-I)). Input: total amount of naïve and dissociated RIG-I applied to the binding assay. The experiment was performed once. (c) Interaction of RIG-I with MAVS was investigated. Naïve RIG-I (insect cells) was incubated with MAVS (ΔTM, Material and methods) in the absence or presence of LMW or HMW poly (I:C) and analysed for MAVS-RIG-I interaction. Interaction between dissociated RIG-I and MAVS was investigated. After 30 min incubation at 37°C, the mixtures were subjected to immunoprecipitation with anti-MAVS, followed by

immunoblotting with anti-Flag (RIG-I) and anti-MAVS. Input: total amount of RIG-I subjected to the assay. The experiment was performed twice. A clear interaction between MAVS and dissociated RIG-I was observed in the two experiments, whereas interaction between naïve RIG-I and MAVS was detectable in neither experiment.

3.6 Function of dissociated RIG-I as the antiviral signaling inducer.

To demonstrate that dissociate RIG-I is the sole signaling molecule for activation of the transcription factor IRF-3 and subsequent *IFNB* gene, dissociated RIG-I was directly introduced to living cells by protein transfection. Cell-derived naïve and dissociated RIG-I were prepared (Materials and methods). Figure 10a shows quantification of the prepared RIG-I by SDS PAGE followed by immunoblotting. The amount of RIG-I was determined from band intensities by using standard recombinant protein as reference. To verify oligomeric status of the cell-derived RIG-I protein, naïve and dissociated RIG-I were analysed by native-PAGE Figure 10b. The result showed that naïve and dissociated RIG-I, which I prepared, are mostly monomeric and oligomeric forms, respectively.

To confirm the physiological ability of dissociated RIG-I in cells, 293T cells were transfected with a reporter plasmid containing 8 repeats IRF-3 binding sites[4,35] prior to transfection of dissociated RIG-I. Then, 293T cells were transfected with cell -derived naive RIG-I or dissociated RIG-I. Cells treated with transfection reagent were used as negative control (MOCK). MOCK treatment and naïve RIG-I transfection exhibited basal reporter gene activity. However, cells transfected with dissociated RIG-I exhibited increased reporter gene expression (Figure 11a).

It has been well documented that IRF-3 undergoes Ser386 phosphorylation[37,38], dimerization and nuclear translocation upon viral infection which triggers the activation of RIG-I. 293T cells were transfected with RIG-I proteins and endogenous IRF-3 was analysed by native-PAGE (Figure 11b). IRF-3 dimer was induced in cells

transfected with dissociated RIG-I, but not with naïve RIG-I. To exclude the possibility that the observed induction of reporter gene and IRF-3 activation were due to contaminated poly (I:C), dissociated RIG-I was treated with RNase III to remove any residual poly (I:C) (Figure 11c) and examined for its ability to activate endogenous *IFNB* gene (Figure 11d). Under these conditions, 30 min RNase III treatment eliminated poly (I:C) to undetectable levels. Lastly the RIG-I proteins treated with or without RNase III were transfected to 293T cells and induction of endogenous *IFNB* gene was examined. Protein transfection of dissociated RIG-I efficiently activated *IFNB* gene, and this activity was resistant to RNase III treatment of the dissociated RIG-I (Figure 11d). Taken together, these results support the hypothesis that naive RIG-I is progressively activated by going through steps of association to dsRNA and dissociation from RIG-I/dsRNA complexes in ATP hydrolysis- dependent manner.

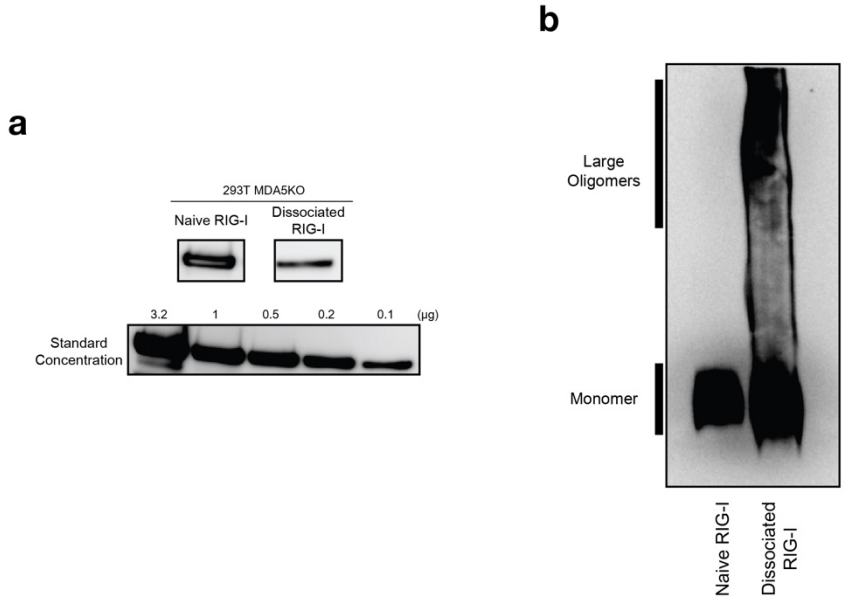

Figure 10. Analysis of 293T cell-derived naïve RIG-I and dissociated RIG-I. (a) Concentration of MDA5KO 293T-derived naive RIG-I and dissociated RIG-I was confirmed by comparison with standard concentration. Naive RIG-I (insect cells), which have already been measured concentration was used as reference. The experiment was performed once. (b) Native PAGE analysis of naïve RIG-I and dissociated RIG-I used for protein transfection (Figure 11). Naïve RIG-I and dissociated RIG-I isolated from MDA5 KO 293T cells were subjected to native PAGE and analyzed by immunoblotting by anti-Flag. The positions of monomers and large oligomers are indicated. The experiment was performed once.

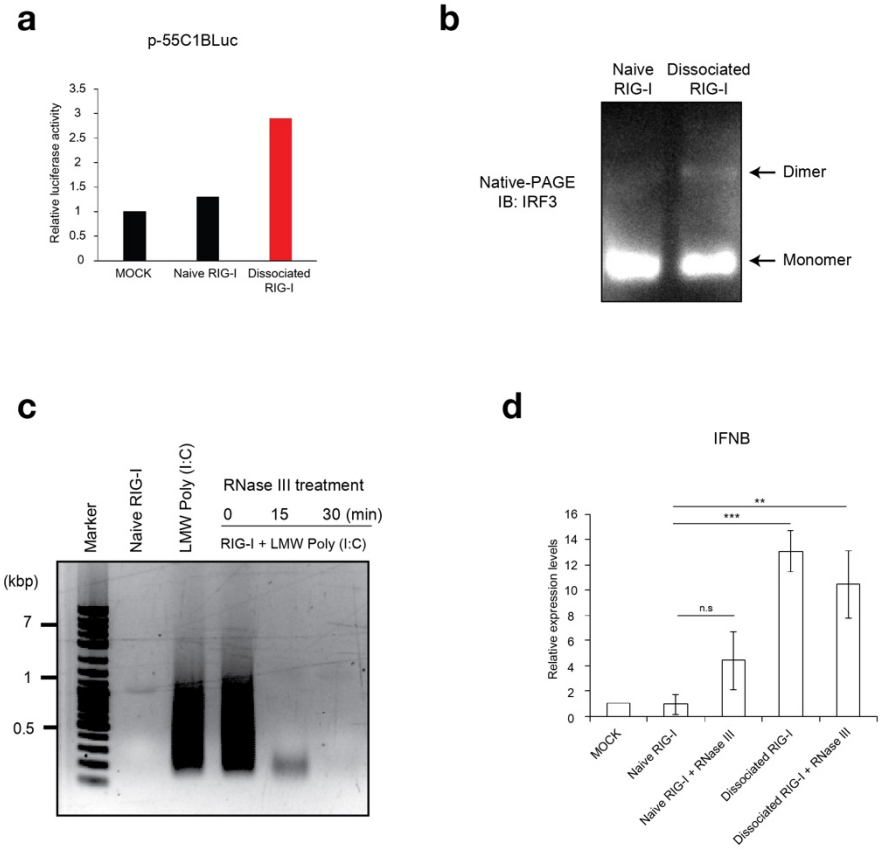

Figure 11. The effect of direct introduction of dissociated RIG-I into mammalian cells. (a) Using reporter gene, p-55C1BLuc, containing repetitive IRF3 binding sites, and pRL-TK, physiological activity of dissociated RIG-I was investigated. Twenty-four hours after transfection of reporter plasmids, cells were directly transfected with 1 μg of naïve or dissociated RIG-I derived from MDA5 KO 293T cells (figure 10), by protein transfection reagent, and incubated for 2 hrs (Material and methods). After additional 4 hrs cultivation with fresh medium, cell lysates were prepared for checking luciferase activity. Relative firefly luciferase activity normalized by Renilla luciferase activity is shown. The experiment was performed with duplicated samples, and total three-independent experiments were performed . A representative data of three independent experiments was expressed as mean values (n=2). (b) The cell extracts were analyzed by native-PAGE for IRF-3 dimer formation. The positions of monomers and dimers are indicated. The experiment was performed once. (c) Setting up conditions for efficient elimination of LMW poly (I:C) by RNase III treatment. A mixture of naïve RIG-I and LMW poly (I:C) (2 μg) was digested with for 15 and 30 min and poly (I:C) was detected by agarose gel electrophoresis. Poly (I:C) was fully digested to undetectable level by 30 min digestion. The experiment was performed once. (d) Naïve or dissociated RIG-I (figure 10) was untreated or treated with RNase III for 30 min and transfected into HeLa cells. The expression level of *IFNB* was analyzed by real-time qPCR. The experiment was performed once with triplicated transfections (in 3 culture wells).

Relative gene expression was calculated as means ± SD (n = 3). Data were analyzed using one-way ANOVA followed by Tukey's post-hoc test (n.s = not significant, **P < 0.01, ***P < 0.001).

Chapter 4

Discussion

Discussion

Since the discovery of RLRs[4], many reports were published describing several classes of RNAs as agonists for these receptors. RLRs are expressed ubiquitously in almost all tissues. RLR knockout mice revealed that RIG-I plays essential function in fibroblast and cDC for detecting viral infection to induce type 1 IFN[2]. Moreover, infection studies of knockout mice revealed that RLRs play essential function in immune response against viruses[3]. Furthermore, RIG-I senses many different RNA and DNA viruses and MDA5 senses specific viral infections including that of picornavirus[30–32,39]. Notably, synthetic poly (I:C), a commonly used viral RNA mimic, acts as specific agonist for MDA5. In summary, RLRs are the biologically critical sensor for viral dsRNA detection and subsequent promotion of antiviral immunity.

In 2006, it was reported that RNA synthesized by *in vitro* transcription by phage RNA polymerase acts as agonist for RIG-I[21,22]. Because 5'-ppp structure was essential for the in vitro transcripts to activate RIG-I, these reports concluded that RIG-I senses 5'-ppp containing ssRNA. However, in 2009, another studies[23,24] corrected the conclusion that in vitro transcription produces copy back dsRNA by phage RNA polymerase using transcript RNA as template. In fact, chemically synthesized 5'-ppp containing ssRNA did not activate RIG-I. Therefore, 5'-ppp structure itself is not sufficient for activating RIG-I, but additional dsRNA structure is important. Furthermore, a short dsRNA (25 bp) without 5'-ppp was shown to activate RIG-I[14]. Also, short poly (I:C) molecules generated by RNAseⅢ do not possess 5'-ppp and termini are either 5'-OH or 3'-p. Collectively, to become an agonist of RIG-I,

dsRNA structure is essential, but 5'ppp structure is optional. However, not all type of dsRNA can trigger antiviral signaling initiated from RIG-I. Earlier report[25] clearly demonstrated that RIG-I and MDA5 sense short and long dsRNA, respectively, but RIG-I is possible to induce active signals by binding short dsRNA, and the mechanism of RIG-I not being activated by binding to long dsRNA was still elusive.

I first confirmed dsRNA size-dependent recognition by RIG-I. I used commercial poly (I:C) (>7 kbp) as dsRNA to generate shorter poly (I:C) species. Because previous studies used natural or synthetic dsRNA, use of poly (I:C) can exclude nucleotide sequence-specific events. Figure 4a reproduced previous report that RNase III is useful to generate different sizes of poly (I:C) [25]. Also, I used human HeLa cells, which express both RIG-I and MDA5. To focus on the function of RIG-I, I used siRNA-mediated knockdown system (Figure 4b). This siRNA has been used in my laboratory and effective to reduce MDA5 expression. I repeated the siRNA validation at least twice and similar results were obtained. Figure 4c suggested that RIG-I is more efficiently activated by shorter poly (I:C) in HeLa cells. I performed this experiment once, however the result is consistent with previous report using wt, RIG-I-/- and MDA5-/- mouse embryonic fibroblasts [25], suggesting that short dsRNA-dependent RIG-I activation of RIG-I is common to mouse and human cells. Next, I reproduced previous observation that RIG-I bound to dsRNA alters its conformation[14]. The report demonstrated that RIG-I protein alone is hypersensitive to trypsin digestion and thoroughly digested by trypsin treatment. However, RIG-I bound with agonistic dsRNA (25 bp), induced trypsin-resistant 30 kDa fragment. In contrast, RIG-I bound to long poly (I:C), larger trypsin-resistant fragment, 66 kDa was induced. In this study,

I examined the effect of chain length of poly (I:C) for induction of 30 and 66 kDa fragments (Figure 4d). The result showed that long and short poly (I:C) preferentially induced 66 and 30 kDa fragments, respectively. This result was reproducible in repeated experiments. The result is consistent with my interpretation that long poly (I:C) does not activate RIG-I not simply due to lack of binding, but RIG-I conforms non-active structure. On the other hand, I interpret that agonistic dsRNA including short poly (I:C), if bound with RIG-I, can induce an ”activated” conformation.

Next, I examined binding kinetics of RIG-I with LMW and HMW poly (I:C) (Figure 5). This result was reproducible in repeated experiments. The result showed that RIG-I bound to LMW poly (I:C) more efficiently than with HMW poly (I:C). Previous studies demonstrated that RIG-I initiate binding with dsRNA from its termini. Devarkar *et al*. demonstrated that restricted modification of dsRNA termini into deoxy nucleotides inhibited RIG-I binding[17]. Peisley *et al*. synthesized dsRNA with single-stranded gap as below. RIG-I specifically bound around the termini but did not occupy beyond the gap, suggesting that RIG-I initiates binding with dsRNA at the termini and translocates along the length of dsRNA[16].

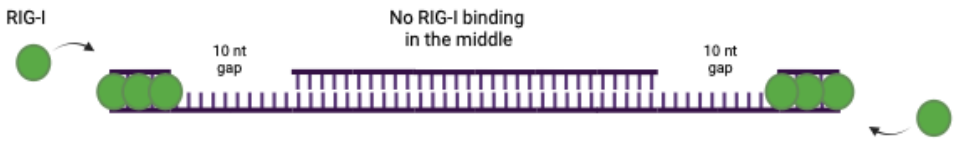

These reports, in agreement, suggested that RIG-I initiate binding from termini and progress binding by scanning through the dsRNA. Based on this notion, I interpret the result of Figure 5 as follows. Because same mass of LMW and HMW poly (I:C)

was used for binding, the termini of LMW poly (I:C) was more abundant, therefore facilitated binding with RIG-I. Under the conditions of Figure 5, 17.5 times higher number of termini was present in LMW poly (I:C) (average 400 bp) compared to HMW poly (I:C) (average 7 kb).

Next, dsRNA length-dependent RIG-I dissociation rate from RIG-I/dsRNA was investigated (Figure 6a). This result was reproducible in repeated experiments. RIG-I was rapidly released from RIG-I/LMW dsRNA complexes, and it was accelerated by ATP hydrolysis (Figure 7). In contrast, RIG-I/HMW poly (I:C) complex remained relatively stable (Figure 6a). AFM imaging of the RIG-I/HMW poly (I:C) complex showed that RIG-I formed large aggregates on HMW poly (I:C). Similar structures were observed in the analyses of RIG-I and natural long dsRNA (genomic dsRNA of Endornaviruses, of rice bran and green pepper, 14-17 kbp) in my independent experiment and in our laboratory (R. Yoshimura Master's thesis). Because HMW poly (I:C) binds with RIG-I but not activate RIG-I, these dsRNA associated aggregates likely represent biologically inactive form of RIG-I (Figure 12). The mechanism for the inactive RIG-I aggregate formation remains to be elucidated. Based on the notion that RIG-I initiates binding from termini of dsRNA and scan along dsRNA[17,18], I propose a model for higher dissociation rate of RIG-I /LMW poly (I:C) (Figure 12). Once RIG-I binds to a terminus, it should translocate to reach to the other terminus to dissociate without being detached from middle of dsRNA and due to short length, the rate of dissociation from termini is higher with short dsRNA.

Above results inspired me that dissociated RIG-I is responsible for signaling to activate antiviral program. I aimed to characterize dissociated RIG-I. First, I used

AFM for molecular imaging of RIG-I molecules (Figure 8). I determined naïve RIG-I image one time (volume 314.86 nm^3) and the result was consistent with previous observation for naïve RIG-I from High five cells (volume, 382.7 nm^3, R. Yoshimura, Master's thesis). Dissociated RIG-I as determined two independent observations revealed significant large size compared to naïve RIG-I (Figure 8). Next, naïve, and dissociated RIG-I was subjected to biochemical analyses (Figure 9). Native-PAGE revealed that dissociated RIG-I is composed of large oligomeric fraction which is missing in naïve RIG-I (Figure 9a), suggesting that RIG-I dissociation from dsRNA is not a simple reversion but irreversible process presumably accompanied with its conformational changes. Consistent with this, dissociated RIG-I did not show binding with LMW poly (I:C) (Figure 9b). Furthermore, dissociated RIG-I, but not naïve RIG-I physically associated with the signal adaptor, MAVS (Figure 9c). These results suggested that the dissociated RIG-I is the activated form for antiviral signal.

To examine dissociated RIG-I is capable of activating IFN promoter, promoter activation assay using a reporter construct driven by repeated IRF binding motifs (p-55C1Bluc) was performed (Figure 11a). The result, which was reproducible in 3 repeated experiments, showed that transfection of dissociated RIG-I alone is sufficient for the activation of the IRF-3 driven promoter. Also, transfection of dissociated RIG-I resulted in IRF-3 dimer formation (Figure 11b), a hallmark event in RIG-I-activation in cells. Although, this experiment was performed once, the result suggest that the reporter gene activation is mediated by IRF-3 activation. Finally, transfection of dissociated RIG-I activated expression of endogenous *IFNB* gene (Figure 11d). In

summary, it is strongly suggested that dissociated RIG-I is the activated form and responsible for activation of MAVS and subsequent *IFNB* gene activation.

CARD of RIG-I if artificially overexpressed, can induce antiviral signal[4]. Indeed, previous report demonstrated that artificially generated CARD oligomers can induce RIG-I activation in absence of dsRNA in living cells[40]. In naïve RIG-I, negative mechanisms maintain repressive state with masked CARD: the "pincer" structure in RIG-I maintains repressive state of RIG-I[41]. Artificially oligomerized RIG-I in cells was sufficient to induce activated signal in an ATP and dsRNA independent manner, suggesting oligomerization of naïve RIG-I is suppressed by yet unknown mechanism (Figure 13, performed by prof. Yoneyama). Collectively, conversion from repressive structure to oligomerized formation is critical for activation of RIG-I. In the current study, the results suggested that naïve RIG-I maintains monomeric or small oligomeric state. However, RIG-I underwent dramatic changes through association to and dissociation from dsRNA: i) formation of large oligomers (Figure 8 and 9a), ii) strong physical interaction with MAVS (Figure 9c), iii) loss of dsRNA binding affinity (Figure 9c). The current notion provides novel mechanism of RIG-I activation by interaction with pathogen associated molecule patterns (PAMPS, in this case dsRNA) to cast RIG-I into active conformation, a process mediated by ATP hydrolysis and final release of the activated RIG-I for downstream signal.

RIG-I and MDA5 sense viral dsRNA with common and unique mechanisms. In the absence of viral RNAs, RIG-I retains repressive conformation, but MDA5 shows stretched conformation like being ready for signal transmission. MDA5 forms fiber-

like complex with long dsRNA and dissociates from dsRNA under the support of LGP2 and ATP hydrolysis[27]. On the other hand, in the case of RIG-I, efficient association and dissociation through dsRNA termini is critical for signal. Therefore, distinct mechanism of sensing viral RNA by RIG-I and MDA5 enable to detect various viral dsRNA.

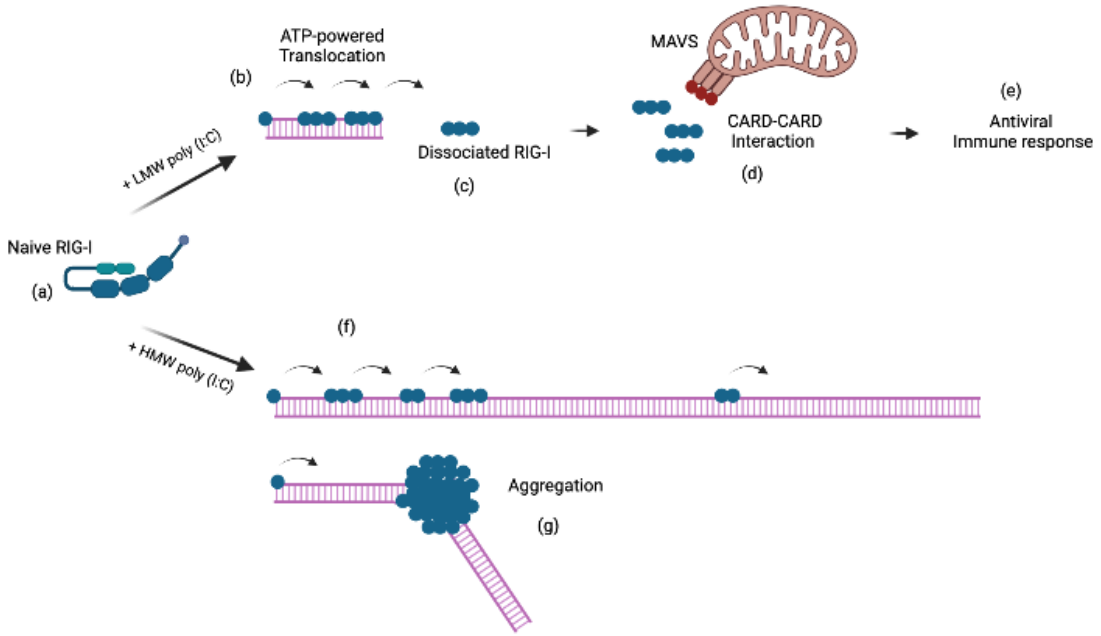

Figure 12. Mechanistic model of RIG-I activation by dsRNA recognition (a) Naïve RIG-I mostly maintains repressive structure including masked CARD in cytoplasm. (b) When RIG-I recognizes LMW dsRNA, RIG-I initiates association to dsRNA through termini of RNA. RIG-I translocates along dsRNA, and the translocation is supported by ATP hydrolysis. (c) At another end of RNA, RIG-I dissociated from LMW dsRNA as oligomerized conformation. (d) Dissociated RIG-I oligomers interact to MAVS, localized on mitochondria, resulting in MAVS oligomerization and recruitment of downstream signaling molecules. (e) The antiviral signaling is induced, such as, IFN-β signals. (f) When RIG-I recognizes HMW dsRNA, RIG-I initiates binding with slower kinetics because of limited number of termini. (g) In middle of translocation on HMW dsRNA, RIG-I binds each other and forms irregular aggregates that block its translocation and dissociation.

.

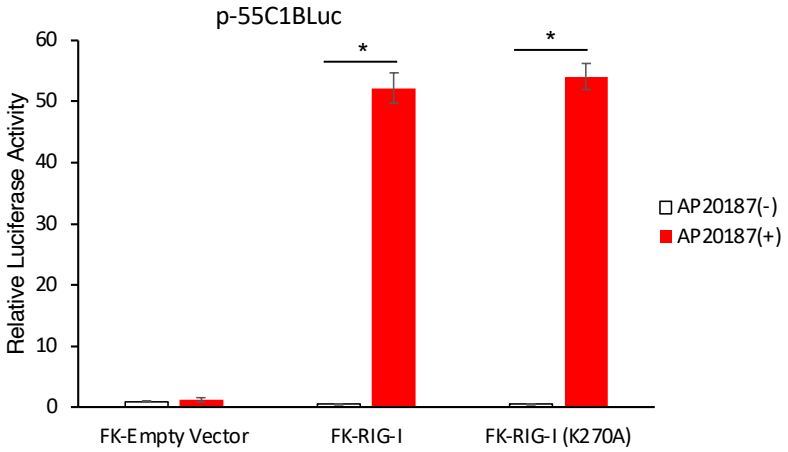

Figure 13. Effect of artificial oligomerization on virus-inducible promoter activation. A fusion construct for 3 tandem repeats of FKBP and full-length human RIG-I was prepared. Another fusion construct for FKBP and RIG-I with disrupted ATP binding site (RIG-I K270A) was similarly prepared. L929 cells were transfected with indicated expression vector and reporter genes, p-55C1BLuc and p-RL-TK. Cells were stimulated by the addition of crosslinker AP20187 for 9 h and luciferase activities were measured (Material and methods). Data of duplicate assays are presented. Error bars represent standard deviation. * $P < 0.05$, two-tailed Student's *t*-test.

Chapter 5

Bibliography

Bibliography

1. Yoneyama, M. *et al.* Shared and Unique Functions of the DExD/H-Box Helicases RIG-I, MDA5, and LGP2 in Antiviral Innate Immunity. *The Journal of Immunology* **175**, 2851–2858 (2005).
2. Kato, H. *et al.* Cell type-specific involvement of RIG-I in antiviral response. *Immunity* **23**, 19–28 (2005).
3. Kato, H. *et al.* Differential roles of MDA5 and RIG-I helicases in the recognition of RNA viruses. *Nature* **441**, 101–105 (2006).
4. Yoneyama, M. *et al.* The RNA helicase RIG-I has an essential function in double-stranded RNA-induced innate antiviral responses. *Nature Immunology* **5**, 730–737 (2004).
5. Andrejeva, J. *et al.* The V proteins of paramyxoviruses bind the IFN-inducible RNA helicase, mda-5, and inhibit its activation of the IFN-β promoter. *Proceedings of the National Academy of Sciences of the United States of America* **101**, 17264–17269 (2004).
6. Rothenfusser, S. *et al.* The RNA Helicase Lgp2 Inhibits TLR-Independent Sensing of Viral Replication by Retinoic Acid-Inducible Gene-I. *The Journal of Immunology* **175**, 5260–5268 (2005).
7. Saito, T. *et al.* Regulation of innate antiviral defenses through a shared repressor domain in RIG-1 and LGP2. *Proceedings of the National Academy of Sciences of the United States of America* **104**, 582–587 (2007).
8. Kawai, T. *et al.* IPS-1, an adaptor triggering RIG-I- and Mda5-mediated type I interferon induction. *Nature Immunology* **6**, 981–988 (2005).

9. Seth, R. B., Sun, L., Ea, C. K. & Chen, Z. J. Identification and characterization of MAVS, a mitochondrial antiviral signaling protein that activates NF-κB and IRF3. *Cell* **122**, 669–682 (2005).

10. Takahasi, K. *et al.* Solution structures of cytosolic RNA sensor MDA5 and LGP2 C-terminal domains: Identification of the RNA recognition loop in RIG-I-like receptors. *Journal of Biological Chemistry* **284**, 17465–17474 (2009).

11. Satoh, T. *et al.* LGP2 is a positive regulator of RIG-I- and MDA5-mediated antiviral responses. *Proceedings of the National Academy of Sciences of the United States of America* **107**, 1512–1517 (2010).

12. Yoneyama, M., Onomoto, K., Jogi, M., Akaboshi, T. & Fujita, T. Viral RNA detection by RIG-I-like receptors. *Current Opinion in Immunology* **32**, 48–53 (2015).

13. Rehwinkel, J. & Gack, M. U. RIG-I-like receptors: their regulation and roles in RNA sensing. *Nature Reviews Immunology* **20**, 537–551 (2020).

14. Takahasi, K. *et al.* Nonself RNA-Sensing Mechanism of RIG-I Helicase and Activation of Antiviral Immune Responses. *Molecular Cell* **29**, 428–440 (2008).

15. Ramanathan, A. *et al.* The autoinhibitory CARD2-Hel2i Interface of RIG-I governs RNA selection. *Nucleic Acids Research* **44**, 896–909 (2016).

16. Peisley, A., Wu, B., Yao, H., Walz, T. & Hur, S. RIG-I Forms Signaling-Competent Filaments in an ATP-Dependent, Ubiquitin-Independent Manner. *Molecular Cell* **51**, 573–583 (2013).

17. Devarkar, S. C., Schweibenz, B., Wang, C., Marcotrigiano, J. & Patel, S. S. RIG-I Uses an ATPase-Powered Translocation-Throttling Mechanism for

Kinetic Proofreading of RNAs and Oligomerization. *Molecular Cell* **72**, 355-368.e4 (2018).

18. Myong, S. *et al.* Cytosolic viral sensor RIG-I is a 5'-triphosphate-dependent translocase on double-stranded RNA. *Science* **323**, 1070–1074 (2009).
19. Kumar, H. *et al.* Essential role of IPS-1 in innate immune responses against RNA viruses. *Journal of Experimental Medicine* **203**, 1795–1803 (2006).
20. Loo, Y.-M. *et al.* Distinct RIG-I and MDA5 Signaling by RNA Viruses in Innate Immunity. *Journal of Virology* **82**, 335–345 (2008).
21. Hornung, V. *et al.* 5′-Triphosphate RNA is the ligand for RIG-I. *Science* **314**, 994–997 (2006).
22. Pichlmair, A. *et al.* RIG-I-mediated antiviral responses to single-stranded RNA bearing 5′-phosphates. *Science* **314**, 997–1001 (2006).
23. Schmidt, A. *et al.* 5′-triphosphate RNA requires base-paired structures to activate antiviral signaling via RIG-I. *Proceedings of the National Academy of Sciences of the United States of America* **106**, 12067–12072 (2009).
24. Schlee, M. *et al.* Recognition of 5′ Triphosphate by RIG-I Helicase Requires Short Blunt Double-Stranded RNA as Contained in Panhandle of Negative-Strand Virus. *Immunity* **31**, 25–34 (2009).
25. Kato, H. *et al.* Length-dependent recognition of double-stranded ribonucleic acids by retinoic acid-inducible gene-I and melanoma differentiation-associated gene 5. *Journal of Experimental Medicine* vol. 205 1601–1610 at https://doi.org/10.1084/jem.20080091 (2008).

26. Marques, J. T. *et al.* A structural basis for discriminating between self and nonself double-stranded RNAs in mammalian cells. *Nature Biotechnology* **24**, 559–565 (2006).

27. Duic, I. *et al.* Viral RNA recognition by LGP2 and MDA5, and activation of signaling through step-by-step conformational changes. *Nucleic Acids Research* **48**, 11664–11674 (2020).

28. Funabiki, M. *et al.* Autoimmune Disorders Associated with Gain of Function of the Intracellular Sensor MDA5. *Immunity* **40**, 199–212 (2014).

29. Berke, I. C. & Modis, Y. MDA5 cooperatively forms dimers and ATP-sensitive filaments upon binding double-stranded RNA. *EMBO Journal* **31**, 1714–1726 (2012).

30. Saito, T. & Gale, M. Differential recognition of double-stranded RNA by RIG-I-like receptors in antiviral immunity. *Journal of Experimental Medicine* **205**, 1523–1527 (2008).

31. Onomoto, K., Onoguchi, K., Takahasi, K. & Fujita, T. Type I interferon production induced by RIG-I-like receptors. *Journal of Interferon and Cytokine Research* **30**, 875–881 (2010).

32. Onoguchi, K., Yoneyama, M. & Fujita, T. Retinoic acid-inducible Gene-I-Like receptors. *Journal of Interferon and Cytokine Research* **31**, 27–31 (2011).

33. Takahasi, K. *et al.* Identification of a new autoinhibitory domain of interferon-beta promoter stimulator-1 (IPS-1) for the tight regulation of oligomerization-driven signal activation. *Biochemical and Biophysical Research Communications* **517**, 662–669 (2019).

34. Abe, H. *et al.* Priming Phosphorylation of TANK-Binding Kinase 1 by IkappaB Kinase beta Is Essential in Toll-Like Receptor 3/4 Signaling. *Mol Cell Biol* **40**, 1–14 (2020).

35. Fujita, T., Shibuyà, H., Hotta, H., Yamanishi, K. & Taniguchi, T. Interferon-β gene regulation: Tandemly repeated sequences of a synthetic 6 bp oligomer function as a virus-inducible enhancer. *Cell* **49**, 357–367 (1987).

36. Takamatsu, S. *et al.* Functional Characterization of Domains of IPS-1 Using an Inducible Oligomerization System. *PLoS ONE* **8**, (2013).

37. Yoneyama, M. *et al.* Direct triggering of the type I interferon system by virus infection : activation of a transcription factor complex containing IRF-3 and CBP / p300. **17**, 1087–1095 (1998).

38. Mori, M. *et al.* Identification of Ser-386 of Interferon Regulatory Factor 3 as Critical Target for Inducible Phosphorylation That Determines Activation. *Journal of Biological Chemistry* **279**, 9698–9702 (2004).

39. Kato, H., Takahasi, K. & Fujita, T. RIG-I-like receptors: Cytoplasmic sensors for non-self RNA. *Immunological Reviews* **243**, 91–98 (2011).

40. Ouda, R. *et al.* Retinoic acid-inducible gene I-inducible miR-23b inhibits infections by minor group rhinoviruses through down-regulation of the very low density lipoprotein receptor. *Journal of Biological Chemistry* **286**, 26210–26219 (2011).

41. Kageyama, M. *et al.* 55 Amino acid linker between helicase and carboxyl terminal domains of RIG-I functions as a critical repression domain and

determines inter-domain conformation. *Biochemical and Biophysical Research Communications* **415**, 75–81 (2011).

Chapter 6

Acknowledgements

Acknowledgements

Thanks to all Fujita lab members, I could complete my research.

Specially thanks to Professor Fujita. He introduced RIG-I protein and guided me to innate immune field. Thanks to his massive knowledges and experiment technique, I was able to try lots of interesting experiments. Especially, his attitude towards research always inspires me not to lose my own way.

Also, thanks to Professor Shige H. Yoshimura, allowed me to use AFM machine.

I appreciate to Ivana for helping me to plan RIG-I experiments and teaching experiments including AFM, protein purification, Seong-Wook Oh for advice and support, and Koshiba-san, who is working for lab as secretary, for many helps. I appreciate to Prof. Noda and three referees for great helps for reviewing my thesis. I could study how to present scientific results correctly and how to make precise statistical analysis.

Lastly, I sincerely appreciate my family for always giving me unstinting support and love.

This study was supported by research grants from Japan Agency for Medical Research and Development: Research Program on Emerging and Re-emerging Infectious Diseases [jp19fk0108081h1001, jp20fk0108081h1202 to F.T.]; Japan Society for the Promotion of Science; Fund for the Promotion of Joint International Research: Fostering Joint International Research (B) [18KK0232 to F.T.]; Core to Core Program: Grant-in-Aid for Scientific Research 'B' [18H02344 to F.T.]. It was also funded by the Deutsche Forschungsgemeinschaft (German Research Foundation) under Germany's Excellence Strategy–EXC2151–390873048 and TRR237, and Deutsche Forschungsgemeinschaft (DFG, German Research Foundation) EXC 2151: ImmunoSensation2, Project number 390873048; DFG TRR 237, Project number 369799452 (B22). Funding for open access charge: DFG ImmunoSensation2.

.

This thesis is based on the material contained in the following scholarly paper:

Mechanisms of length-dependent recognition of viral double-stranded RNA by RIG-I

Jung Hyun Im, Ivana Duic, Shige H. Yoshimura, Koji Onomoto, Mitsutoshi Yoneyama, Hiroki Kato and Takashi Fujita

Scientific Reports, Nature Portfolio, volume 13, article number 6318

Published: 18 April 2023
DOI: 10.1038/s41598-023-33208-w